We are IntechOpen, the world's leading publisher of Open Access books Built by scientists, for scientists

4,800
Open access books available

122,000
International authors and editors

135M
Downloads

Our authors are among the

154
Countries delivered to

TOP 1%
most cited scientists

12.2%
Contributors from top 500 universities

CLARIVATE ANALYTICS
BOOK CITATION INDEX
INDEXED

WEB OF SCIENCE™

Selection of our books indexed in the Book Citation Index
in Web of Science™ Core Collection (BKCI)

Interested in publishing with us?
Contact book.department@intechopen.com

Numbers displayed above are based on latest data collected.
For more information visit www.intechopen.com

Experiments and Models of Thermo-Induced Shape Memory Polymers

Qianhua Kan, Jian Li, Guozheng Kang and
Zebin Zhang

Additional information is available at the end of the chapter

Abstract

Recent advances in experiments and models of thermo-induced shape memory polymers (TSMPs) were reviewed. Some important visco-elastic and visco-plastic features, such as rate-dependent and temperature-dependent stress-strain curves and nonuniform temperature distribution were experimentally investigated, and the interaction between the mechanical deformation and the internal heat generation was discussed. The influences of loading rate and peak strain on the shape memory effect (SME) and shape memory degeneration of TSMPs were revealed under monotonic and cyclic thermo-mechanical loadings, respectively. Based on experimental observations, the capability of recent developed visco-elastic and visco-plastic models for predicting the SME was evaluated, and the thermo-mechanically coupled models were used to reasonably predict the thermo-mechanical responses of TSMPs.

Keywords: shape memory polymers, thermo-mechanical coupling, constitutive models, glassy transition, relaxation

1. Introduction

Thermo-induced shape memory polymers (TSMPs) are one of most widely applicable shape memory polymers (SMPs) at present, which exhibit the shape memory effect (SME) by changing the ambient temperature. TSMPs are different from the traditional polymers; some of their important features related to the SME were summarized by Lendlein et al. [1] and Hager et al. [2] as follows: (1) a phase presents the rubber-like state in a wide temperature range above the glassy transition temperature (T_g) and has a stable strength to deform; (2) a
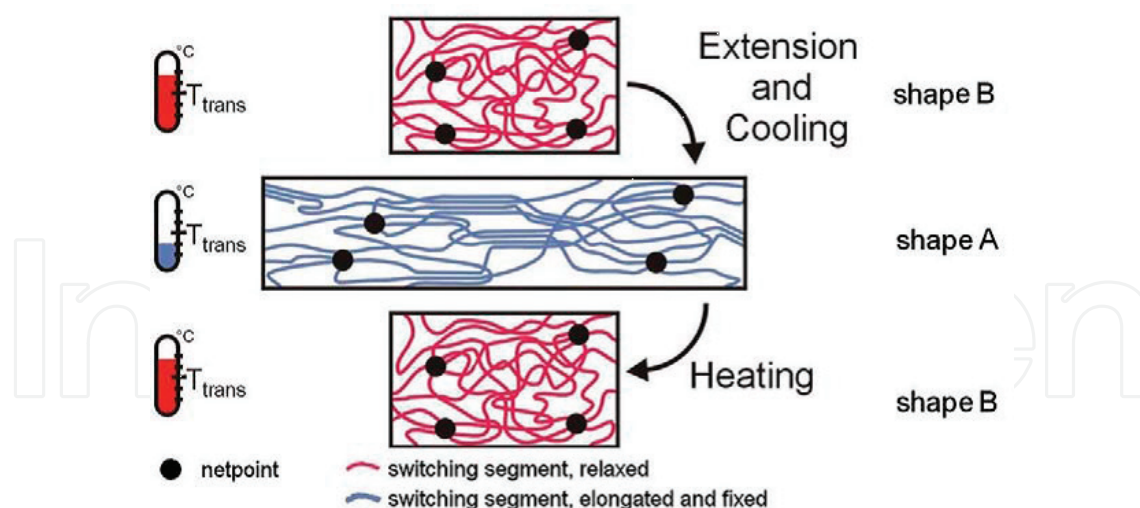
Figure 1. The molecular mechanism of the SME of TSMPs [3].

phase presents the glass-like state in a wide temperature range below T_g and has a stable strength to ensure that the internal stress is not be released in storage; (3) The two separable phases are the structural basis of SME and the suitable ratio between the two phases should be existent. The molecular mechanism of TSMPs was presented by Behl et al. [3], as shown in **Figure 1**. There are three parts in TSMPs, including the netpoint, the relaxed switching segment, the elongated and fixed switching segment (i.e., the transition phase, it can transform between the netpoint and the relaxed switching segment with the change of temperature).

The popular topics focus on the fabrications, the analysis of mechanisms and applications of TSMPs [3–5]. The constitutive models describing the glassy transition mechanism of TSMPs are summarized and they can be divided into two types according to different deformation mechanisms, including the thermo-visco-elastic rheology model and the meso-mechanical model [6]. The thermo-visco-elastic model can describe the mobility of chain segments and relaxation with temperature by introducing the relaxation time and the temperature-dependent modulus. The meso-mechanical model adopted a mixture rule of rubber and glassy phases by the volume fractions of frozen and active phases. For considering the interaction between the internal heat generation and mechanical deformation, the thermo-mechanically coupled models were developed by introducing different dissipation mechanisms.

In this chapter, recent advances in experiments and models of TSMPs are reviewed. According to experimental observations, some deformation mechanisms and features of TSMPs are summarized. The capability of two types of models in predicting the mechanical responses and the SME of TSMPs are evaluated, and some interesting issues and further developments of TSMPs were discussed in the end.

2. Experiment observations

2.1. Mechanical performances

The mechanical properties of TSMPs are strongly sensitive to the ambient temperature and the loading rate and can be obtained from tensile experiments at different temperatures and loading rates, as shown in **Figure 2**.

It is found from **Figure 2** that the high-stress responses at low temperature is a typical feature of amorphous polymers, and the low stress responses at high temperature is a typical feature of visco-elastic polymer. The yield peak gradually disappears when the temperature goes beyond the glassy transition temperature T_g.

The thermo-mechanical properties can be obtained from the dynamic mechanical analysis (DMA) [7]. As shown in **Figure 3**, the storage and loss moduli obtained from DMA are found as functions of temperature. The glassy transition temperature, where the ratio of loss modulus and storage modulus (tan δ) dramatically changes, can be obtained from the DMA results, and the glassy transition temperature increases with the frequency [8]. In addition, the glassy transition temperature can be also obtained from the differential scanning calorimeter (DSC) test [9].

2.2. Thermo-mechanical coupling behaviors

The thermo-mechanical coupling behaviors are divided into two types here, one is that the mechanical behavior changes with the ambient temperature, that is, SME; the other is the temperature changes induced by the internal heat generation.
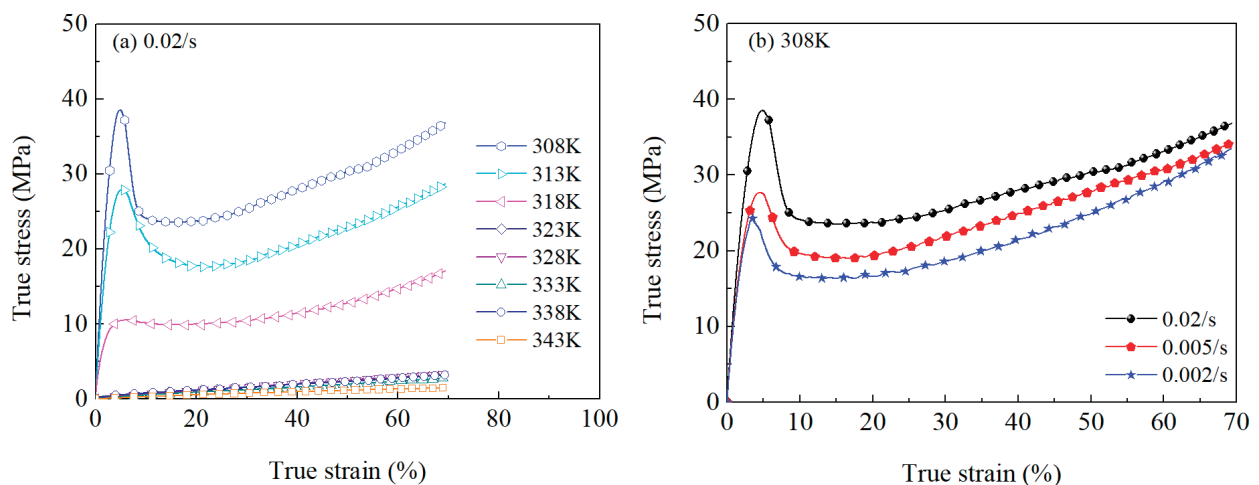
Figure 2. Stress-strain curves of monotonic tension at (a) different temperatures and (b) loading rates.
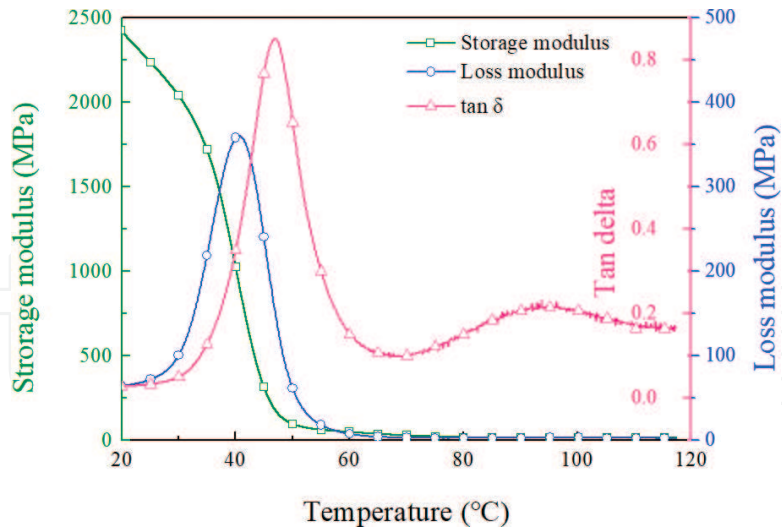
Figure 3. The curves of storage modulus, loss modulus, and tanδ versus temperature.
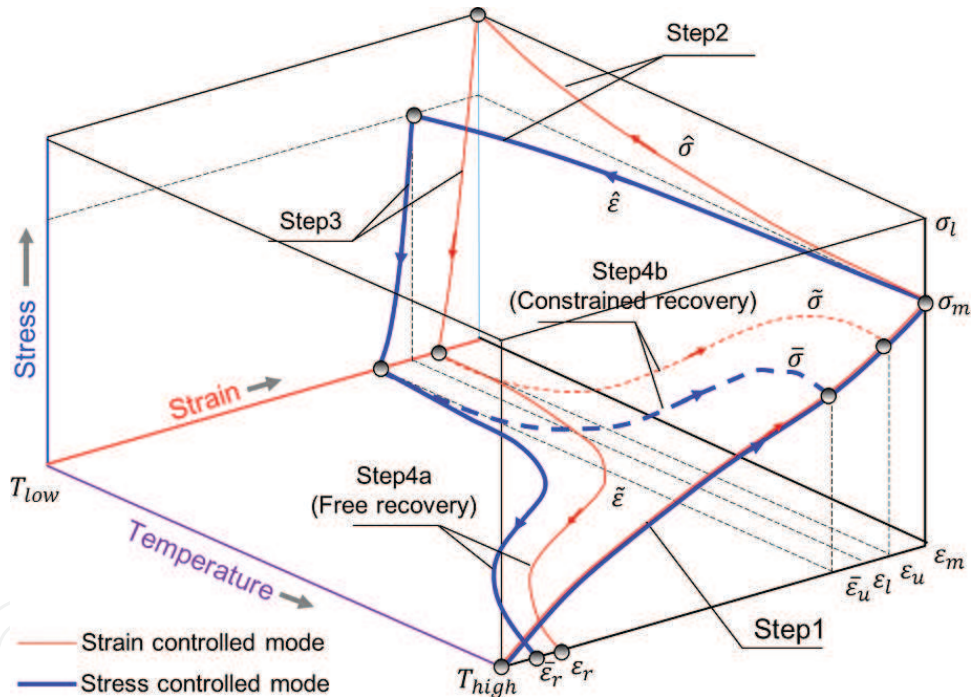

Figure 4. The illustration of SME of TSMPs.

2.2.1. Shape memory effect

As shown in **Figure 4**, a typical SME process includes four stages, that is, Step1: deforming at high temperature above T_g; Step2: cooling to the storage temperature (room temperature in general); Step3: unloading at the storage temperature and the shape is fixed; Step4: heating to the recoverable temperature above T_g, the deformed shape returns to the initial undeformed shape.

The SME process can be divided into stress-controlled (stress-free recovery) and strain-controlled (strain-constraint recovery) modes during strain recovery by heating, respectively. Two parameters are usually used to character the SME, including the shape fixity ratio R_f and the shape recovery ratio R_r [10, 11] as shown in Eqs. (1) and (2).

$$R_f = \frac{\varepsilon_u}{\varepsilon_m} \times 100 \tag{1}$$

$$R_r = \frac{\varepsilon_m - \varepsilon_r}{\varepsilon_m} \times 100 \tag{2}$$

where ε_m, ε_u and ε_r denote the peak strain, fixed strain and residual strain, respectively.

Besides, the recoverable glassy transition temperature in the stress-free recovery, the maximum recovery stress in the constraint recovery and the recoverable temperature at the maximum recovery stress are also used to quantify the SME [10–13].

The experimental results of TSMPs sheet (MM4520) at different strain rates and peak strains are shown in **Figure 5**.

It is found from **Figure 5** that the maximum stress at the cooling stage decreases with the increase of loading rate, and the shape recovery ratio of TSMPs in the stress-free recovery decreases with the increase of peak strain and the decrease of strain rate, which is similar with shape memory experiments of TSMPs sheet (MS4510) [14]. It is the reason that the viscosity increases with the increase of strain rate and the damage in chain segments increases with the increase of peak strain. The correlation between the loading rate and the shape recovery ratio can be explained, as the relaxation of the stored elastic energy is easier at low loading rate than at high loading rate. However, the SME in the stress-free recovery is independent on the peak strain; the recovery maximum stress increases with the increase of peak strain for the aliphatic polyether urethane [13].

In the molecular level, a prior orientation of switching chain segments of thermoplastic TSMPs improves with the increase of macroscopic deformation; once these chain segments return to the random coil-like conformation, the maximum recovery stress increases in the strain-constraint recovery. However, the peak strain has almost no influence on the SME for the
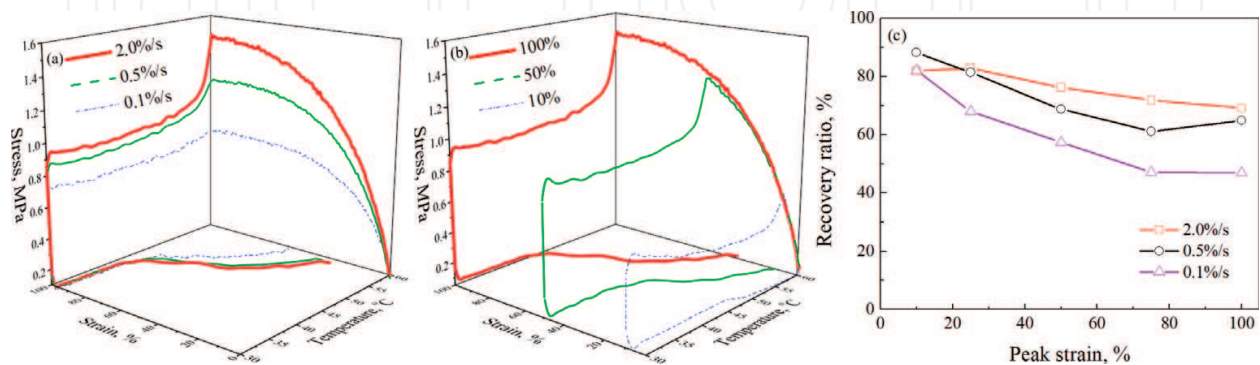
Figure 5. Stress-strain-temperature curves at different (a) strain rates, (b) peak strains, and (c) shape recovery ratio versus peak strain at different strain rates.

thermoset TSMPs [12, 15] since the thermoset TSMPs have a more stable molecular structure than the thermoplastic TSMPs.

Hu et al. [14] found that TSMPs film (MS4510) exhibits an excellent SME at the temperature range from T_g to T_g + 25°C, and the shape recovery ratio decreases beyond the temperature range. To obtain better SME in practical applications, the TSMPs film should be cooled to its frozen state as soon as possible after being deformed at high temperature. Cui and Lendlein [13] found the switching temperature of shape recovery in the stress-free recovery, the maximum recovery stress and the corresponding temperature in the strain-constraint recovery increase with the increase of deformation temperature. The start temperature of shape recovery can be controlled by adjusting the cooling temperature during unloading [16].

Besides, many factors can remarkably affect the shape recovery ratio, for example, the shape recovery ratio decreases with the increase of holding time after deformation since the increase of holding time causes a large relaxation of the stored elastic energy [17, 18]. The shape recovery ratio increases with the increase of finish recovery temperature since the mobility of chain segments is more active at high temperature [14, 18]. If the recovery temperature is higher than the deformation temperature, the inactive chain segments during the deforming stage can be activated to increase their mobility. The shape recovery ratio increases with the decrease of heating rate since the heat conduction of TSMPs requires enough time. If the holding time increases after approaching the finish recovery temperature, the effect of heating rate on the shape recovery ratio can be eliminated [15].

According to the experiment results, the mobility of chain segments, visco-elasticity, stress relaxation and structural relaxation of TSMPs also have influences on the SME. These influential factors change with temperature and can be utilized to optimize the SME.

2.2.2. Internal heat generation induced by deformation

TSMPs are sensitive to the temperatures, including the temperature caused by the internal heat generation and ambient temperature. According to the thermo-mechanically coupled experiments [8, 19, 20], an infrared camera is used to measure the surface temperature of TSMPs for indicating the interaction between mechanical deformation and temperature. It is concluded that TSMPs are very sensitive to the temperature and loading rate, and the temperature localization is related to the strain localization, as shown in **Figures 6–8**. The temperature firstly decreases during the elastic deformation stage and then increases during visco-plastic deformation stage in tension, which implies that the internal heat generation is contributed by two parts, that is, the decreased temperature due to the thermo-elastic effect and the increased temperature due to the visco-plastic dissipation. It is noted from **Figure 7** that the temperature variation increases with the increase of loading rate and it can be explained as with the increase of loading rate in tension, the resistance of the slipping of chain segments increases, which results in a larger dissipation caused by the friction of disentanglement of chain segments.

The stress-strain curves and temperature variations of TSMPs subjected to loading-unloading mechanical cycles were obtained by Pieczyska et al. [20], as shown in **Figure 9**. It is found that the residual strain accumulates and the amplitude of temperature variation decreases with the
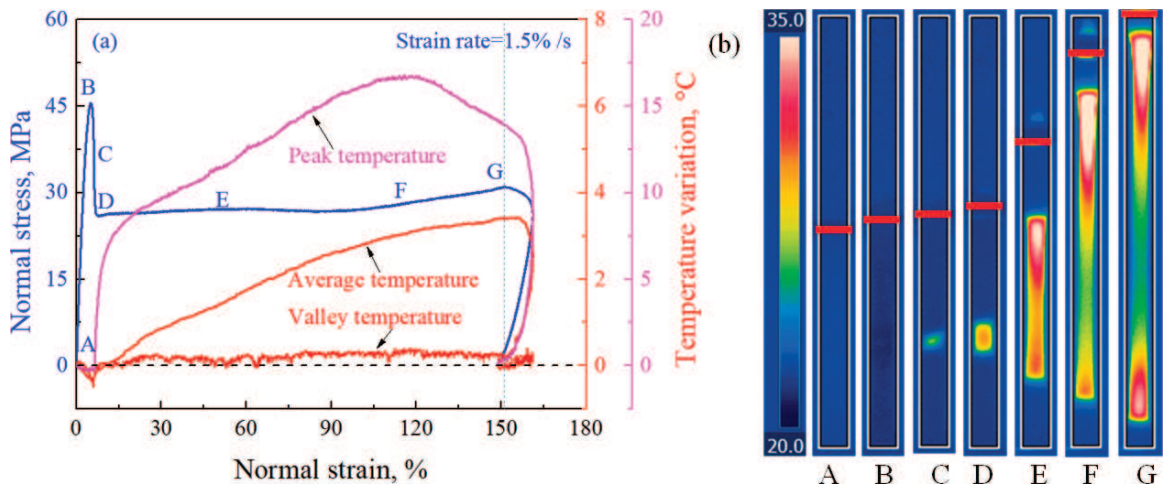
Figure 6. (a) Curves of stress-strain and strain-temperature variation; and (b) temperature field distribution.
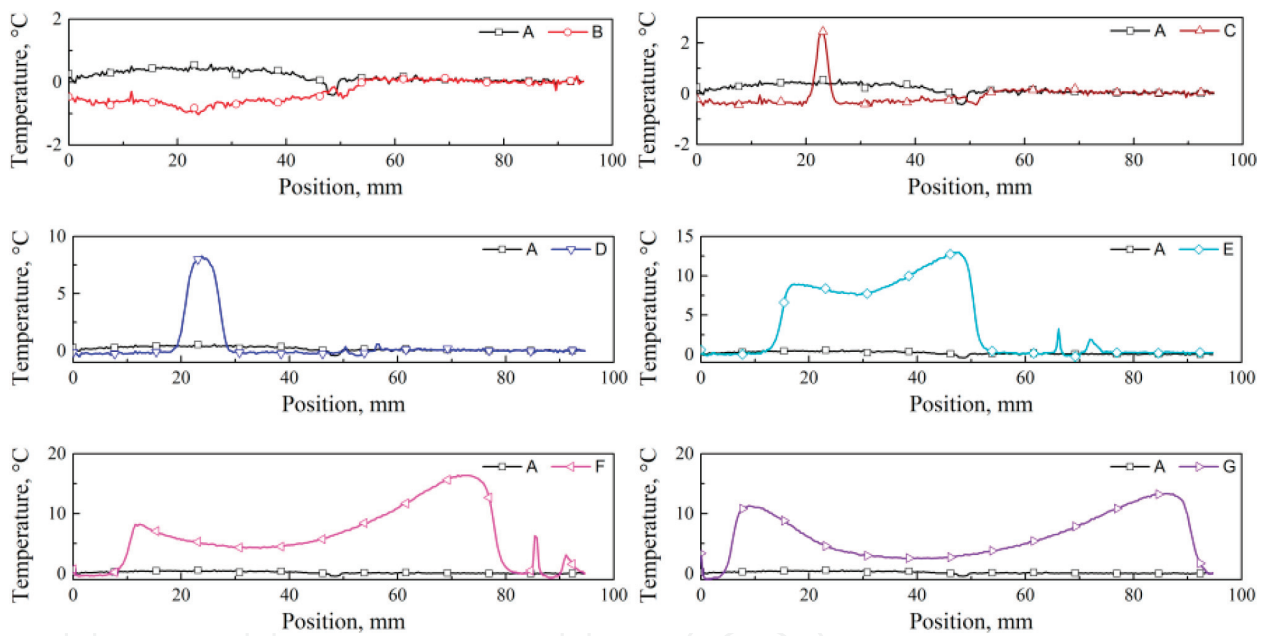

Figure 7. Curves of temperature versus position corresponding to **Figure 6(b)**.

increase of number of cycles. It is the reason that the decreased stress at peak strain due to the stress relaxation and the accumulated residual strain after unloading result in a narrower and narrower hysteresis loop, that is, decreased visco-plastic dissipation with the increase of number of cycles.

2.3. Shape memory degradation

When the TSMPs are subjected to thermo-mechanical cyclic loadings (i.e., repeated shape memory cycles), the shape memory degradation can be characterized by the strain recovery rate R_{rate} [11, 21] and strain recovery ratio R_{ratio} [22], respectively, as below:
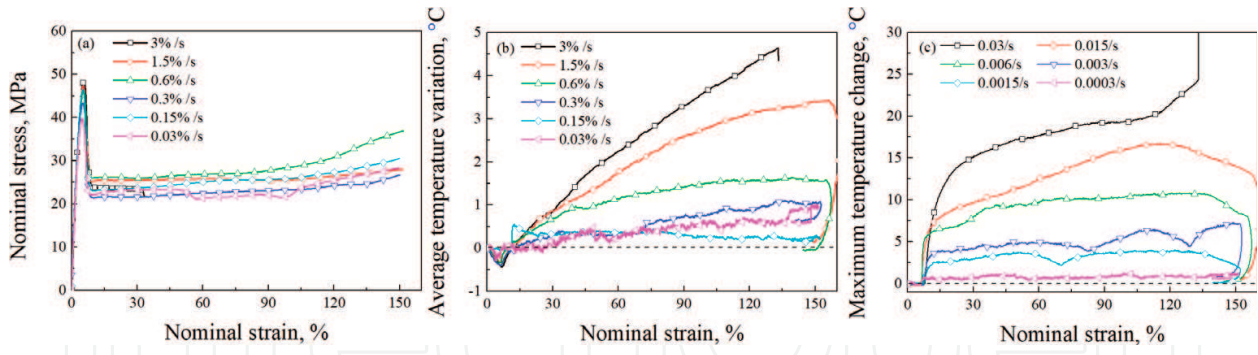
Figure 8. (a) Stress-strain curves; (b) curves of average temperature variation versus strain; and (c) curves of maximum temperature variation versus strain.
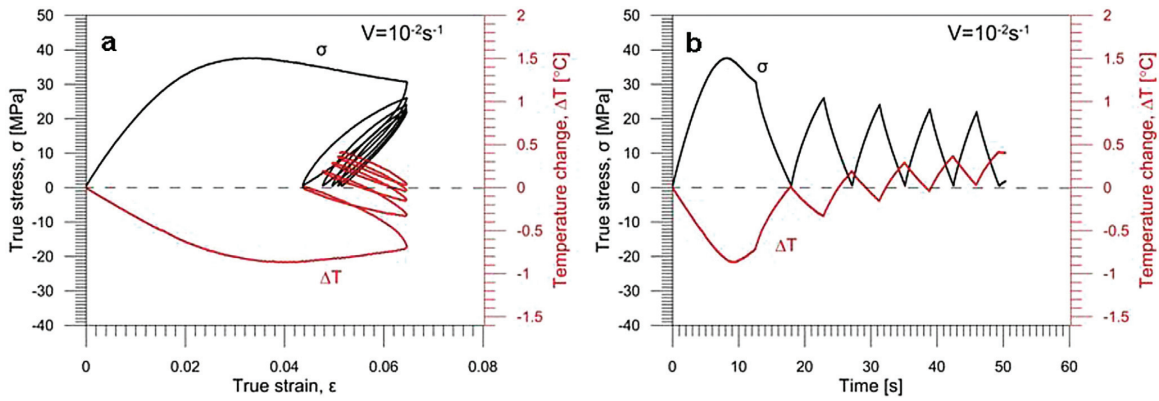

Figure 9. Stress and temperature change of TSMPs subjected to loading-unloading cycles versus (a) true strain and (b) time [20].

$$R_{\text{rate}}(N) = \frac{\varepsilon_u(N) - \varepsilon_r(N)}{\varepsilon_u(N) - \varepsilon_r(N\text{-}1)} \times 100 \qquad (3)$$

$$R_{\text{ratio}}(N) = \frac{\varepsilon_m - \varepsilon_r(N)}{\varepsilon_m} \times 100 \qquad (4)$$

where ε_m denotes the peak strain during loading, $\varepsilon_u(N)$ and $\varepsilon_r(N)$ denote the fixed strain and residual strain after unloading in the N-th cycle, respectively.

The experimental results subjected to shape memory cycles are shown in **Figure 10** [11, 22]. It is found that the strain recovery rate gradually increases with the decrease of peak strain and the increase of number of cycles and rapidly approaches 100% after several cycles. However, the recovery strain ratio depends on the peak strain, for example, it increases with the increase of peak strain; however, it decreases when the peak strain is up to 150%.

The shape memory degeneration also depends on the deformable temperature, recovery temperature and mechanical training [22–25]. For example, as shown in **Figure 11**, the strain
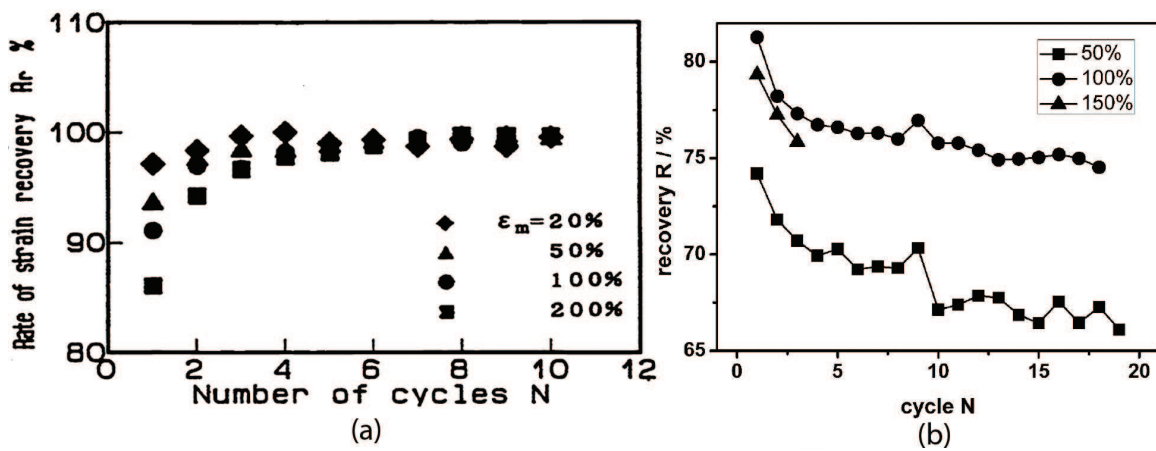
Figure 10. Curves of (a) the strain recovery rate [11] and (b) the strain recovery ratio [22] with number of cycles.
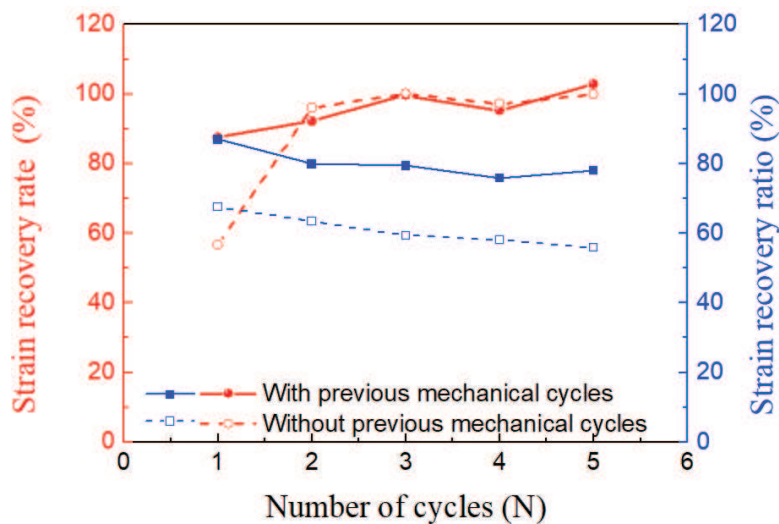

Figure 11. The influences of previous mechanical cycles on the strain recovery rate and strain recovery ratio [25].

recovery ratio of TSMPs can be improved by undergoing previous mechanical cycles since the mechanical training can eliminate the heterogeneous structure of chain segments [24]. However, the previous mechanical cycles have almost no influence on strain recovery rate.

2.4. Novel experimental observations on SME

Conventional experimental methods limited within uniaxial tension or compression were discussed in Sections 2.1–2.3. Recently, many advanced experimental methods and complex loading modes were developed to investigate the SME of TSMPs. For example, the nano-indentation technology was used to examine the SME of TSMPs, and the indentation can be recovered by heating the sample to above the glass transition temperature [26]; this research provides a foundation to explore the nano-mechanical behavior of TSMPs.

The shear deformation and its recovery behavior were investigated through a double lap joint arrangement at below and above T_g [27]. Torsional shape memory tests were carried out to characterize the SME, and a torsional device with a CCD camera was used to quantify the parameters of the SME [28]. A series of tension, compression, bending and twisting experiments of TSMPs were performed to indicate the SME; it is shown that the heating rate has an obvious influence on the start temperature of shape recovery [29].

These experimental findings provide an experimental guidance for future applications, including aerospace, automotive, robotics, and smart actuator, and so on. Some novel experiments and protocols are expected to be designed for characterizing the SME of smart structures in future.

3. Constitutive models

Constitutive models of TSMPs, including shape memory model describing the SME and the thermo-mechanically coupled model describing the internal heat generation caused by mechanical deformation, are commented on in this section.

3.1. Shape memory model

Based on the different deformation mechanisms, different models were constructed to describe the SME of TSMPs, including the rheology model considering the mobility and relaxation and the meso-mechanical model considering the phase transition between the frozen and active phases.

3.1.1. Rheology model

The mobility of chain segments is a classical mechanism to describe the SME, which remarkably depends on ambient temperature. Tobushi et al. [21] think that the shape of TSMPs can be fixed due to the decreased mobility of chain segments with the decrease of temperature, and the shape can be recovered due to the increased mobility of chain segments with the increase of temperature. Therefore, a rheological model was proposed by introducing a slip element into a three-element standard linear visco-elastic model, as shown in **Figure 12**, and the mobility of chain segments can be expressed as the exponential functions between material parameters and temperature, as shown in Eq. (5).

$$x(T) = \begin{cases} x(T_l) & (T \leq T_l) \\ x_g \exp\left[a_x\left(\dfrac{T_g}{T} - 1\right)\right] & (T_l \leq T \leq T_h) \\ x(T_h) & (T \geq T_h) \end{cases} \quad (x = E, \mu, \lambda, C, \varepsilon_l) \quad (5)$$

where, σ, ε and ε_l denote the stress, strain and irrecoverable strain, E is elastic modulus. μ and λ are viscosity and retardation time, respectively. C is a coefficient of irrecoverable strain. T, T_l, T_g, T_h and a_x denote the current temperature, low temperature, glassy transition temperature, melting temperature and proportional coefficient, respectively.
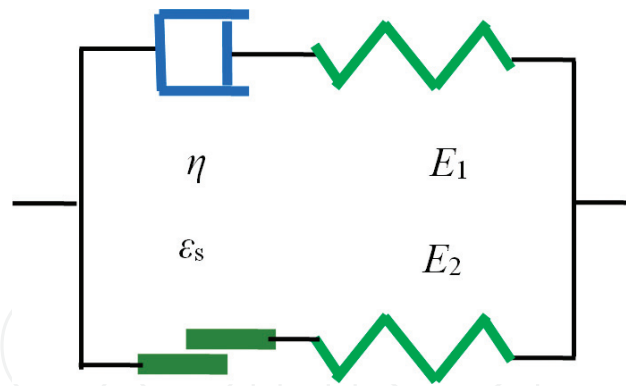
Figure 12. Four-element model.

To describe the nonlinear behaviors of TSMPs, a one-dimensional nonlinear visco-elastic model was extended from a linear visco-elastic version [30]. However, the extended model provides an overestimation of the responded stress at large strain, and thus the linear model was further modified to reasonably simulate the SME of TSMPs at large strain by introducing new nonlinear evolution equations with stress threshold values into the cooling modulus and irrecoverable strain [31].

It is noted that, even though the mechanical responses at large strain were simulated, the abovementioned models were established at small deformation. Therefore, Diani et al. [32] developed a thermo-mechanical model of TSMPs at finite deformation based on the three element standard linear visco-elastic model [21]. The total deformation gradient is decomposed into elastic and viscous parts. The total Cauchy stress includes the stresses caused by the entropy change and internal energy change, respectively.

Nguyen et al. [33] developed a thermo-visco-elastic model to describe the time-dependent and temperature-dependent deformations of TSMPs by incorporating structural relaxation and stress relaxations. The model can reproduce the strain-temperature response, rate-dependent stress-strain response and some important features of temperature dependent shape memory responses. In the model, a fictive temperature T_f is used to describe the structural relaxation behavior and the structural relaxation time is obtained from the WLF equation, as shown in Eq. (6). The stress relaxation adopts the form of visco-elasticity in the glass transition region and rubbery state, and the modified WLF equation is introduced into the Eyring equation to obtain a modified visco-plastic flow rule for describing the visco-plastic deformation, including the glassy state and rubbery state, see Eq. (7).

$$\tau_R\left(T, T_f\left(\overline{\delta}^{neq}\right)\right) = \tau_{Rg} \exp\left[-\frac{C_1}{\log e}\left(\frac{C_2(T - T_f) + T\left(T_f - T_g^{ref}\right)}{T\left(C_2 + T_f - T_g^{ref}\right)}\right)\right] \tag{6}$$

$$\dot{\gamma}^v = \frac{s_y}{\sqrt{2}\eta_{s_g}^{ref}}\frac{T}{Q_s} \exp\left[\frac{C_1}{\log e}\left(\frac{C_2(T - T_f) + T\left(T_f - T_g^{ref}\right)}{T\left(C_2 + T_f - T_g^{ref}\right)}\right)\right] \sinh\left(\frac{Q_s}{T}\frac{\|s^{neq}\|}{\sqrt{2}s_y}\right) \tag{7}$$

where τ_R and τ_{Rg} are the structural relaxation time and relaxation time at a reference temperature T_g^{ref}, respectively; C_1 and C_2 are material constants using in the WLF equation. $\overline{\delta}^{neq}$ denotes the nonequilibrium part of the isobaric volumetric deformation. $\dot{\gamma}^v$ and s_y denote the effective viscous shear stretch rate and yield strength. Q_s is a thermal activation parameter and $\mathbf{s}^{neq}$ is the nonequilibrium part of the deviatoric component of Cauchy stress.

Based on the model proposed by Nguyen et al. [33], Li et al. [7] also developed a thermo-visco-elastic-visco-plastic model considering the structural relaxation and stress relaxation. The model was used to predict the nonlinear SME of TSMPs programmed by cold-compression below the glassy transition temperature. Chen et al. [34] performed parameter studies on the SME in the conditions of the stress-free recovery and strain-constrained recovery with different loading parameters, including the cooling rate, heating rate, strain rate, anneal time and temperature. The results show that the SME is affected by different mechanisms, including the thermal expansion, structural relaxation and stress relaxation. Chen et al. [35] developed a rheological model by introducing the thermal expansion, structural relaxation and stress relaxation into a standard linear visco-elastic model; the Mooney-Rivlin function and Newton fluid assumptions were used to describe the hyper-elasticity of rubbery state and flow behavior of glassy state during the process of the glass transition, respectively.

Recently, the multibranch models considering the stress relaxation were developed to reasonably capture the SME of TSMPs [16, 36–38]. For considering more complex shape memory behaviors, Xiao et al. [39] proposed a thermo-visco-plastic model at finite deformation to describe the multiple SME and temperature memory effect by introducing the structural relaxation and stress relaxation [39]. Besides, for the purpose of the structural analysis, the linear visco-elastic model [21] was extended to three-dimensional version and was implemented into ABAQUS by using the user material subroutine UMAT to simulate the SME of structures [40–43].

3.1.2. Meso-mechanical model

The meso-mechanical model was firstly proposed by Liu et al. [44] to describe the physical mechanisms of the stress-free recovery and strain-constraint recovery at the pre-deformation strain level of TSMPs. In the model, it is assumed that the TSMPs consist of two extreme phases, including the frozen phase and active phase. The frozen phase is the major phase in the glassy state, where the conformational motion is constrained. In contrast, the active phase exists in the full rubbery state, and the free conformational motion potentially occurs. By changing the ratio of these two phases, the glassy transition in a thermo-mechanical cycle is embodied and thus the shape memory effect can be captured. To quantify the changes of mechanical properties with temperature, the volume fraction of frozen phase is defined as Eq. (8) and can be obtained by fitting the curve of recovery strain. It is assumed that the corresponding stresses in these two phases are equal to $\boldsymbol{\sigma}$ (see Eq. (9)), and the total strain $\boldsymbol{\varepsilon}$ is defined as Eq. (10).

$$\phi_f = 1 - \frac{1}{1 + c_f(T_h - T)^n} \tag{8}$$

$$\boldsymbol{\sigma} = \phi_f \boldsymbol{\sigma}_f + (1 - \phi_f)\boldsymbol{\sigma}_a, \ \boldsymbol{\sigma}_f = \boldsymbol{\sigma}_a = \boldsymbol{\sigma} \tag{9}$$

$$\boldsymbol{\varepsilon} = \phi_f \boldsymbol{\varepsilon}_f + (1 - \phi_f)\boldsymbol{\varepsilon}_a \tag{10}$$

where ϕ_f denotes the volume fraction of frozen phase; $\boldsymbol{\sigma}$ is the total stress; $\boldsymbol{\sigma}_a$ and $\boldsymbol{\sigma}_f$ are the stresses in the active phase and frozen phase, respectively; $\boldsymbol{\varepsilon}$ is the total strain; and $\boldsymbol{\varepsilon}_a$ and $\boldsymbol{\varepsilon}_f$ are the strains in the active phase and frozen phase, respectively.

Based on the meso-mechanical model [44], the thermo-elastic models [45, 46] were constructed to simulate the SME of TSMPs at small deformation and large deformation, respectively. Qi et al. [47] assumed that the TSMPs consist of three phases, including the rubbery phase, initial glassy phase and frozen glassy phase. The volume fraction of each phase is assumed as the function of temperature, as shown in Eq. (11). The volume fraction of rubbery phase ϕ_r is defined as Eq. (12) during cooling and heating. The volume fraction of rubbery phase transforms into the volume fraction of frozen glassy phase during cooling. It is assumed that the increments in the volume fractions of the initial glassy phase ϕ_{g0} and frozen glassy phases ϕ_T depend on their relative volume fraction during reheating, as shown in Eq. (12). In the meantime, the corresponding stresses in the three phases satisfy with the rule of mixture, see Eq. (13).

$$\phi_g + \phi_r = 1, \quad \phi_{g0} + \phi_T = \phi_g \tag{11}$$

$$\phi_r = \frac{1}{1 + \exp\left[-(T - T_r)/A\right]}, \, \Delta\phi_{g0} = \frac{\phi_{g0}}{\phi_{g0} + \phi_T}\Delta\phi_g, \, \Delta\phi_T = \frac{\phi_T}{\phi_{g0} + \phi_T}\Delta\phi_g \tag{12}$$

$$\mathbf{T} = \phi_r\mathbf{T}_r + \phi_{g0}\mathbf{T}_{g0} + \phi_T\mathbf{T}_T \tag{13}$$

where $\mathbf{T}$ is the total stress. $\mathbf{T}_r$, $\mathbf{T}_{g0}$ and $\mathbf{T}_T$ denote stress in the rubbery phase, frozen phase and initial glassy phase, respectively.

Based on the abovementioned meso-mechanical method with a mixture rule, a three-dimensional model was proposed for TSMPs [48], which distinguishes between two phases presenting different properties. The model can reproduce both heating-stretching-cooling and cold drawing shape-fixing procedures and was applied in the simulations from simple uniaxial and biaxial tests to complex loadings of biomedical devices.

3.2. Thermo-mechanically coupled model

Pieczyska proposed thermo-mechanically coupled models at finite deformation [8, 19] to reproduce the rate-dependent stress-strain curve and the strain localization behavior. However, this model cannot describe the temperature variation induced by the internal heat generation since the thermo-elastic effect and the visco-plastic dissipation are neglected. To reasonably describe the influence of the internal heat generation on the mechanical behavior of TSMPs, the Helmholtz free energy ψ is decomposed into three parts, that is, the instantaneous elastic free energy ψ^e, visco-plastic free energy ψ^{vp} and heat free energy ψ^T, and the stress-strain relationship is derived from the Helmholtz free energy [49], as shown in Eqs. (14)–(17).

$$\psi(\mathbf{C}^e, \mathbf{B}^{vp}, T) = \psi^e(\mathbf{C}^e, T) + \psi^{vp}(\mathbf{B}^{vp}, T) + \psi^T(T) \tag{14}$$

$$\psi^e(\mathbf{E}^e, T) = G(T)\left|\mathbf{E}_0^e\right|^2 + \frac{1}{2}K(T)|\text{tr}(\mathbf{E}^e)|^2 - 3K(T)\text{tr}(\mathbf{E}^e)\alpha(T - T_0) \tag{15}$$

$$\psi^{\mathrm{vp}}(\lambda^{\mathrm{vp}}, T) = \mu_{\mathrm{R}}(T)\lambda_{\mathrm{L}}^{2}\left[\left(\frac{\lambda^{\mathrm{vp}}}{\lambda_{\mathrm{L}}}\right)x + \ln\left(\frac{x}{\sinh x}\right)\right], \quad x = \mathcal{L}^{-1}\left(\frac{\lambda^{\mathrm{vp}}}{\lambda_{\mathrm{L}}}\right) \tag{16}$$

$$\psi^{T}(T) = c\left[(T - T_0) - T\ln\left(\frac{T}{T_0}\right)\right] + u_0 - \eta_0 T \tag{17}$$

where $\mathbf{C}^{\mathrm{e}}$, $\mathbf{B}^{\mathrm{vp}}$ denote the elastic right Cauchy-Green tensor and visco-plastic left Cauchy-Green tensor, respectively. $\mathbf{E}^{\mathrm{e}}$ and $\mathbf{E}_0^{\mathrm{e}}$ are the Hencky's logarithmic strain and its deviatoric part, respectively. T_0 is the initial temperature. λ^{vp} and λ_L denote the visco-plastic stretch and limiting stretch, respectively. u_0 and η_0 denote the initial internal energy and initial entropy, respectively. μ_R, G and K denote the temperature-dependent hardening modulus, shear modulus and bulk modulus, respectively. The parameter c denotes the specific heat, and the symbol $\mathcal{L}^{-1}$ denotes the inverse of Langevin function.

The heat equilibrium equation of the internal heat generation and heat exchange is derived based on an average temperature filed along the sample, as shown in Eq. (18).

$$c_{\mathrm{eff}}\dot{T} = \omega\Gamma_{\mathrm{eff}} + \frac{h(T_0 - T)S}{V} \tag{18}$$

where h is the heat exchange coefficient of ambient media, which is a constant if without forced convection. c_{eff} and Γ_{eff} are the equivalent specific heat and dissipation, respectively, S and V
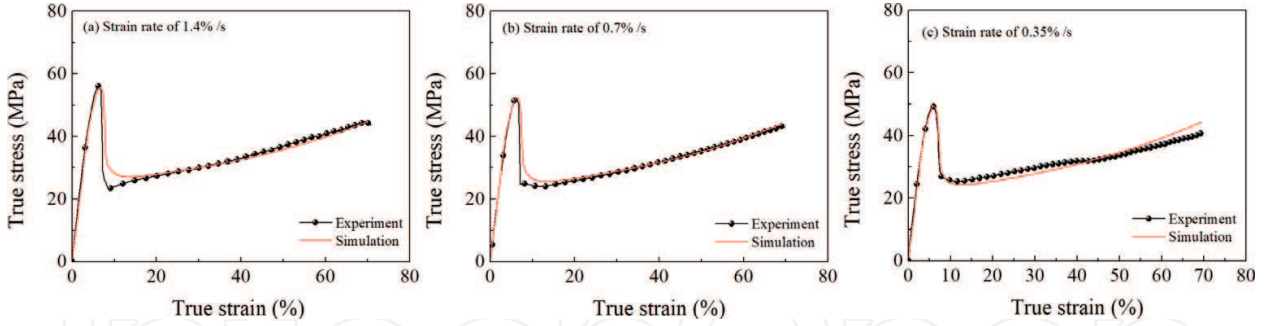

Figure 13. Experimental and simulated stress-strain curves at different strain rates: (a) 1.4%/s; (b) 0.7%/s; and (c) 0.35%/s.
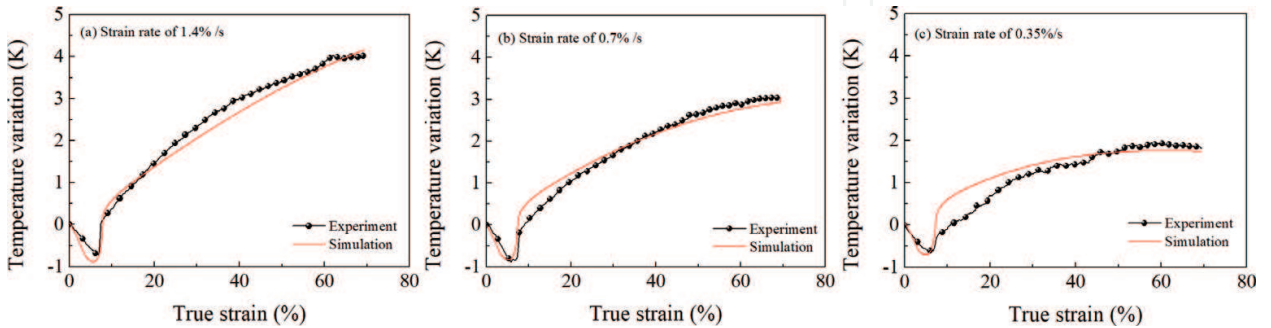

Figure 14. Experimental and simulated temperature variation at different strain rates: (a) 1.4%/s; (b) 0.7%/s; and (c) 0.35%/s.

are the volume and surface of a specimen. The proportional factor $_n$ is introduced to reflect the proportion of the work converting into heat.

Based on the abovementioned constitutive description, a thermo-elasto-visco-plastic model was established at finite deformation to reasonably predict the rate-dependent stress-strain responses and temperature variations, including the temperature drop due to the thermo-elastic effect and the temperature rise due to the visco-plastic dissipation, as shown in **Figures 13** and **14**.

4. Conclusions and remarks

Recent advances in experiments and models of TMPs are reviewed, the main conclusions are below:

1. The TSMPs exhibit rate-dependent and temperature-dependent mechanical responses, a strong interaction between the internal heat generation and mechanical deformation is observed and strain and temperature distributions are nonuniform in tension. The internal heat generation is contributed by the decreased temperature due to the thermo-elastic effect and the increased temperature due to the visco-plastic dissipation.

2. The SME of TSMPs in the conditions of the stress-free recovery and strain-constraint recovery can be characterized by the shape recovery ratio, which decreases with the increases of peak strain, holding time after deformation, heating rate and decrease with the decreases of loading rate and finish recovery temperature.

3. The shape memory degeneration of TSMPs occurs under cyclic thermo-mechanical loadings and can be reflected by the strain recovery ratio, which gradually decreases with the increase of number of cycles and also depends on the peak strain, deformable temperature, recovery temperature and previous mechanical training.

4. Two types of models have been established, including the shape memory model which describing the SME and the thermo-mechanically coupled model which describing the interaction between the mechanical deformation, internal heat generation and heat exchange.

5. As mentioned earlier, most experiments and models of TSMPs are limited within uniaxial loading and the SME is performed by heating to a certain temperature. The experimental observations on the proportional and nonproportional multiaxial mechanical responses and the SME subjected to shape memory cycles are insufficient, the multiaxial thermo-mechanically coupled model is necessary to be constructed for predicting the SME more accurate. Moreover, the experimental and theoretical investigations on the deformation mechanisms of the multiple SME and temperature memory effect are necessary to be addressed in future.

Acknowledgements

Author details

Qianhua Kan[1]*, Jian Li[2], Guozheng Kang[1] and Zebin Zhang[2]

*Address all correspondence to: qianhuakan@foxmail.com

1 State Key Laboratory of Traction Power, Southwest Jiaotong University, Chengdu, P. R. China

2 School of Mechanics and Engineering, Southwest Jiaotong University, Chengdu, P. R. China

References

[1] Lendlein A, Kelch S. Shape-memory polymers. Angewandte Chemie International Edition. 2002;**41**(12):2034-2057. DOI: 10.1007/978-3-642-12359-7

[2] Hager MD, Bode S, Weber C, et al. Shape memory polymers: Past, present and future developments. Progress in Polymer Science. 2015;**49-50**:3-33. DOI: 10.1016/j.progpolymsci.2015.04.002

[3] Behl M, Lendlein A. Shape-memory polymers. Materials Today. 2007;**10**(4):20-28. DOI: 10.1016/S1369-7021(07)70047-0

[4] Leng JS, Lan X, Liu Y, et al. Shape-memory polymers and their composites: Stimulus methods and applications. Progress in Materials Science. 2011;**56**(7):1077-1135. DOI: 10.1016/j.pmatsci.2011.03.001

[5] Hu J, Zhu Y, Huang H, et al. Recent advances in shape–memory polymers: Structure, mechanism, functionality, modeling and applications. Progress in Polymer Science. 2012;**37**(12):1720-1763. DOI: 10.1016/j.progpolymsci.2012.06.001

[6] Nguyen TD. Modeling shape-memory behaviour of polymers. Polymer Reviews. 2013;**53**(1):130-152. DOI: 10.1080/15583724.2012.751922

[7] Li G, Xu W. Thermomechanical behaviour of thermoset shape memory polymer programmed by cold-compression: Testing and constitutive modeling. Journal of the Mechanics & Physics of Solids. 2011;**59**(6):1231-1250. DOI: 10.1016/j.jmps.2011.03.001

[8] Pieczyska EA, Maj M, Kowalczykgajewska K, et al. Thermomechanical properties of polyurethane shape memory polymer-experiment and modelling. Smart Materials & Structures. 2015;**24**(4):045043. DOI: 10.1088/0964-1726/24/4/045043

[9] Zhang ZX, He ZZ, Yang JH, et al. Crystallization controlled shape memory behaviors of dynamically vulcanized poly (l-lactide) /poly (ethylene vinyl acetate) blends. Polymer Testing. 2016;**51**:82-92. DOI: 10.1016/j.polymertesting.2016.03.003

[10] Kim BK, Sang YL, Mao X. Polyurethane having shape memory effect. Polymer. 1996;**37**(26):5781-5793. DOI: 10.1016/S0032-3861(96)00442-9

[11] Tobushi H, Hara H, Yamada E, et al. Thermomechanical properties in a thin film of shape memory polymer of polyurethane series. Smart Materials & Structures. 1996;**2716**(4):483. DOI: 10.1117/12.232168

[12] Atli B, Gandhi F. Thermomechanical characterization of shape memory polymers. Journal of Intelligent Material Systems & Structures. 2009;**17**(20):7002-7011. DOI: 10.1117/12.715248

[13] Cui J, Kratz K, Lendlein A. Adjusting shape-memory properties of amorphous polyether urethanes and radio-opaque composites thereof by variation of physical parameters during programming. Smart Materials & Structures. 2010;**19**(6):065019. DOI: 10.1088/0964-1726/19/6/065019

[14] Hu JL, Ji FL, Wong YW. Dependency of the shape memory properties of a polyurethane upon thermomechanical cyclic conditions. Polymer International. 2005;**54**(3):600-605. DOI: 10.1002/pi.1745

[15] Volk B L, Lagoudas D C, Chen Y C, et al. Analysis of the finite deformation response of shape memory polymers: I. Thermomechanical characterization. Smart Material Structures. 2010;**19**(7):75005-75014(10). DOI: 10.1088/0964-1726/19/7/075005

[16] Zhang C, Gou X, Xiao R. Controllable shape-memory recovery regions in polymers through mechanical programming. Journal of Applied Polymer Science. 2017;**135**(8). DOI: 10.1002/app.45909

[17] Mcclung AJW, Tandon GP, Baur JW. Deformation rate-, hold time-, and cycle-dependent shape-memory performance of Veriflex-E resin. Mechanics of Time-Dependent Materials. 2013;**17**(1):39-52. DOI: 10.1007/s11043-011-9157-6

[18] Azra C, Plummer CJG, Månson JAE. Isothermal recovery rates in shape memory polyurethanes. Smart Materials & Structures. 2011;**20**(8):082002. DOI: 10.1088/0964-1726/20/8/082002

[19] Pieczyska EA, Staszczak M, Maj M, et al. Investigation of thermomechanical couplings, strain localization and shape memory properties in a shape memory polymer subjected to loading at various strain rates. Smart Materials & Structures. 2016;**25**(8):085002. DOI: 10.1088/0964-1726/25/8/085002

[20] Pieczyska EA, Staszczak M, Kowalczyk-Gajewska K, et al. Experimental and numerical investigation of yielding phenomena in a shape memory polymer subjected to cyclic tension at various strain rates. Polymer Testing. 2017;**60**:333-342. DOI: 10.1016/j.polymertesting.2017.04.014

[21] Tobushi H, Hashimoto T, Hayashi S, et al. Thermomechanical constitutive modeling in shape memory polymer of polyurethane series. Journal of Intelligent Material Systems and Structures. 1997;**8**(8):711-718. DOI: 10.1177/1045389X9700800808

[22] Schmidt C, Neuking K, Eggeler G. Functional fatigue of shape memory polymers. Advanced Engineering Materials. 2010;**10**(10):922-927. DOI: 10.1002/adem.200800213

[23] Schmidt C, Chowdhury AMS, Neuking K, et al. Studies on the cycling, processing and programming of an industrially applicable shape memory polymer Tecoflex(R) (or TFX EG 72D). Journal of the Royal Society of Medicine. 2011;**80**(9):544-546. DOI: 10.1177/0954008311405245

[24] Mogharebi S, Kazakeviciute-Makovska R, Steeb H, et al. On the cyclic material stability of shape memory polymer. Materialwissenschaft Und Werkstofftechnik. 2013;**44**(6):521-526. DOI: 10.1002/mawe.201300023

[25] Zhang Z, Li J, Chen K, et al. Experimental observation on the thermo-mechanically cyclic deformation behaviour of shape memory polyurethane. Gongneng Cailiao/journal of Functional Materials. 2017;**48**(5):05174-05179. DOI: 10.3969/j.issn.1001-9731.2017.05.032

[26] Wornyo E, Gall K, Yang F, et al. Nanoindentation of shape memory polymer networks. Polymer. 2007;**48**(11):3213-3225. DOI: 10.1016/j.polymer.2007.03.029

[27] Khan F, Koo JH, Monk D, et al. Characterization of shear deformation and strain recovery behaviour in shape memory polymers. Polymer Testing. 2008;**27**(4):498-503. DOI: 10.1016/j.polymertesting.2008.02.006

[28] Diani J, Frédy C, Gilormini P, et al. A torsion test for the study of the large deformation recovery of shape memory polymers. Polymer Testing. 2011;**30**(3):335-341. DOI: 10.1016/j.polymertesting.2011.01.008

[29] Du H, Liu L, Zhang F, et al. Thermal-mechanical behaviour of styrene-based shape memory polymer tubes. Polymer Testing. 2017;**57**:119-125. DOI: 10.1016/j.polymertesting.2016.11.011

[30] Tobushi H, Okumura K, Hayashi S, et al. Thermomechanical constitutive model of shape memory polymer. Mechanics of Materials. 2001;**33**(10):545-554. DOI: 10.1016/S0167-6636(01)00075-8

[31] Li J, Dong SY, Kan QH, et al. A Thermo-mechanical constitutive model of glassy shape memory polymers. Applied Mechanics & Materials. 2016;**853**:96-100. DOI: 10.4028/www.scientific.net/AMM.853.96

[32] Diani J, Liu Y, Gall K. Finite strain 3D thermoviscoelastic constitutive model for shape memory polymers. Polymer Engineering & Science. 2006;**46**(4):486-492. DOI: 10.1002/pen.20497

[33] Nguyen TD, Qi HJ, Castro F, et al. A thermoviscoelastic model for amorphous shape memory polymers: Incorporating structural and stress relaxation. Journal of the Mechanics and Physics of Solids. 2008;**56**(9):2792-2814. DOI: 10.1016/j.jmps.2008.04.007

[34] Chen X, Nguyen TD. Influence of thermoviscoelastic properties and loading conditions on the recovery performance of shape memory polymers. Mechanics of Materials. 2011;**43**(3):127-138. DOI: 10.1016/j.mechmat.2011.01.001

[35] Chen J, Liu L, Liu Y, et al. Thermoviscoelastic shape memory behaviour for epoxy-shape memory polymer. Smart Materials and Structures. 2014;**23**(5):055025. DOI: 10.1088/0964-1726/23/5/055025

[36] Westbrook KK, Kao PH, Castro F, et al. A 3D finite deformation constitutive model for amorphous shape memory polymers: A multi-branch modeling approach for non-equilibrium relaxation processes. Mechanics of Materials. 2011;**43**(12):853-869. DOI: 10.1016/j.mechmat.2011.09.004

[37] Yu K, Mcclung AJW, Tandon GP, et al. A thermomechanical constitutive model for an epoxy based shape memory polymer and its parameter identifications. Mechanics of Time-Dependent Materials. 2014;**18**(2):453-474. DOI: 10.1007/s11043-014-9237-5

[38] Li Y, He Y, Liu Z. A viscoelastic constitutive model for shape memory polymers based on multiplicative decompositions of the deformation gradient. International Journal of Plasticity. 2017;**91**:300-317. DOI: 10.1016/j.ijplas.2017.04.004

[39] Xiao R, Guo J, Nguyen TD. Modeling the multiple shape memory effect and temperature memory effect in amorphous polymers. RSC Advances. 2014;**5**(1):416-423. DOI: 10.1039/c4ra11412d

[40] Zhou B, Liu Y, Leng J. Finite element analysis on thermo-mechanical behaviour of styrene-based shape memory polymers. Acta Polymerica Sinica. 2009;**009**(6):525-529. DOI: 10.3321/j.issn:1000-3304.2009.06.005

[41] Shi G, Yang Q, He X, et al. A three-dimensional constitutive equation and finite element method implementation for shape memory polymers. Computer Modeling in Engineering & Sciences. 2013;**90**(5):339-358. DOI: 10.3970/cmes.2013.090.339

[42] Shi GH, Yang QS, He XQ. Analysis of intelligent hinged shell structures: Deployable deformation and shape memory effect. Smart Materials & Structures. 2013;**22**(12):126-132. DOI: 10.1088/0964-1726/22/12/125018

[43] Liu YF, Wu JL, Zhang JX, et al. Feasible evaluation of the Thermo-mechanical properties of shape memory polyurethane for orthodontic Archwire. Journal of Medical & Biological Engineering. 2017;**37**(5):666-674. DOI: 10.1007/s40846-017-0263-z

[44] Liu Y, Gall K, Dunn ML, et al. Thermomechanics of shape memory polymers: Uniaxial experiments and constitutive modeling. International Journal of Plasticity. 2006;**22**(2):279-313. DOI: 10.1016/j.ijplas.2005.03.004

[45] Chen YC, Lagoudas DCA. Constitutive theory for shape memory polymers. Part I: Large deformations. Journal of the Mechanics & Physics of Solids. 2008;**56**:1752-1765. DOI: 10.1016/j.jmps.2007.12.005

[46] Chen YC, Lagoudas DC. A constitutive theory for shape memory polymers. Part II : A linearized model for small deformations. Journal of the Mechanics and Physics of Solids. 2008;**56**(5):1766-1778. DOI: 10.1016/j.jmps.2007.12.004

[47] Qi HJ, Nguyen TD, Castro F, et al. Finite deformation thermo-mechanical behaviour of thermally induced shape memory polymers. Journal of the Mechanics & Physics of Solids. 2008;**56**(5):1730-1751. DOI: 10.1016/j.jmps.2007.12.002

[48] Boatti E, Scalet G, Auricchio F. A three-dimensional finite-strain phenomenological model for shape-memory polymers: Formulation, numerical simulations, and comparison with experimental data. International Journal of Plasticity. 2016;**83**:153-177. DOI: 10.1016/j.ijplas.2016.04.008

[49] Li J, Kan Qnnnnn Kang G, et al. Thermo-mechanically coupled thermo-elasto-visco-plastic modeling of thermo-induced shape memory polyurethane at finite deformation. Acta Mechanica Solida Sinica. 2018;**31**(2):141-160. DOI: 10.1007/s10338-018-0022-x